Kidney360

Identification of Podocyte Cargo Proteins by Proteomic Analysis of Clathrin-Coated Vesicles

Marwin Groener,[1,2,3] Ying Wang,[1] Elizabeth Cross,[1] Xuefei Tian,[1] Karen Ebenezer,[1] Eunice Baik,[1] Christopher Pedigo,[1] Mario Schiffer,[2,3,4] Kazunori Inoue,[1] and Shuta Ishibe[1]

Abstract

Background Clathrin-mediated endocytosis (CME) plays a fundamental role in podocyte health. Genetic ablation of genes implicated in CME has been shown to cause severe proteinuria and foot process effacement in mice. However, little is known about the cargo of clathrin-coated vesicles (CCVs) in podocytes. The goal of this study was to isolate CCVs from podocytes and identify their cargo by proteomic analysis.

Methods Glomeruli isolated from *Podocin-Cre Rosa-DTR^{flox}* mouse kidneys were seeded and treated with diphtheria toxin to obtain pure primary podocyte cultures. CCVs were isolated by differential gradient ultracentrifugation, and enrichment of CCVs was assessed by immunoblotting and electron microscopy (EM). Liquid chromatography-mass spectrometry (LC-MS) was performed for proteomic analysis. Proteins with higher abundance than transferrin receptor protein 1 were evaluated for CCV cargo potential against previously published literature. Immunofluorescence staining of identified cargo proteins and CCVs was performed in podocytes for further verification.

Results Immunoblotting for multiple protein markers of CME revealed enrichment in the CCV fraction. Enrichment of CCVs among other small vesicles was observed *via* EM. Proteomics yielded a total of >1200 significant proteins. Multiple-step data analysis revealed 36 CCV-associated proteins, of which 10 represent novel, highly abundant cargo proteins in podocytes. Colocalization of cargo proteins and CCVs on immunostaining was observed.

Conclusions Our identification of podocyte CCV cargo proteins helps to elucidate the importance of endocytic trafficking for podocyte health and maintenance of the glomerular environment.

KIDNEY360 1: 480–490, 2020. doi: https://doi.org/10.34067/KID.0000212020

Introduction

In living cells, endocytosis is a process allowing for uptake of macromolecules and receptors through invagination of the plasma membrane forming vesicles. Endocytosis is often categorized as clathrin-dependent and -independent pathways, and proteins can often exploit either pathway allowing for internalization. In clathrin-mediated endocytosis (CME), cargo proteins bind to adaptor proteins (APs) at the plasma membrane, followed by the creation of a clathrin-coated pit. The clathrin coat is generated by three clathrin heavy chains (CHCs) and three clathrin light chains (CLCs) that form a triskelion, a structure with three arc-shaped "legs" that are connected at a central base. Multiple clathrin triskelions assemble to hexamers and pentamers, resulting in a surface with a convex and concave side (1). Eventually, a spherelike vesicle is formed during clathrin-coated vesicle (CCV) maturation. After vesicle budding through enzymatic scission of the "neck" of the clathrin-coated pit, the CCV and cargo are internalized, and guided to endosomes for recycling or degradation (2). Over 50 years ago, electron microscopy (EM) revealed ultrastructural evidence of endosomal and vesicular structures in the podocyte (3). More recently, the physiologic relevance of this endocytic machinery has been studied (4) and the importance of CME for podocyte health identified. Podocyte-specific genetic ablation in mice for genes critical for CME has resulted in severe proteinuria, suggesting a vital role in maintaining the integrity of the glomerular filtration barrier (5). Furthermore, recent studies identifying human mutations in *GAPVD1*, *ANKFY1*, and *TBC1D8B*, genes critical for endosomal trafficking, have further highlighted the importance of these regulatory pathways (6,7). Under physiologic circumstances, podocytes rely heavily on CME for maintenance of the slit diaphragm for internalizing nephrin (5,8), as well as receptors such as the type Ia angiotensin II receptor (9).

[1]Department of Internal Medicine, Yale University School of Medicine, New Haven, Connecticut
[2]Department of Nephrology and Hypertension, University Hospital Erlangen, Erlangen, Germany
[3]Friedrich-Alexander-Universität Erlangen-Nürnberg (FAU), Erlangen, Germany
[4]Mount Desert Island Biological Laboratories, Salisbury Cove, Maine

Correspondence: Dr. Shuta Ishibe, Section of Nephrology, Yale University School of Medicine, PO Box 208029, 333 Cedar Street, New Haven, CT 06520-8029. Email: shuta.ishibe@yale.edu

However, to our knowledge, CCV proteomics to identify CCV-associated proteins have not been elucidated in podocytes. In order to further identify the proteins that interact with or are internalized by CME, in this study, we isolated primary podocytes, followed by differential centrifugation to enrich for CCVs. The isolated fraction of CCVs underwent organelle proteomics using mass spectrometry (MS) to identify quantitatively CCV-associated proteins within the podocytes. Using multiple-step data analysis, we identified 36 CCV-associated proteins in podocytes, 10 of which represent novel, highly abundant cargo proteins of CCVs. Collectively, these results provide new insights into podocyte CME through the identification of new partners with implications in podocyte health and disease.

Materials and Methods

Antibodies

Antibodies used were mouse anti-CHC (sc-12734; Santa Cruz); rabbit anti-CLC (AB9884; Sigma-Aldrich); rabbit anti-dynamin 2 (a kind gift from Pietro DeCamilli at Yale University); mouse anti-α-adaptin (MA1–064, Invitrogen); rabbit anti-glyceraldehyde 3-phosphate dehydrogenase (#2118; Cell Signaling); mouse anti-transferrin receptor (13–6800; Life Technologies); rat anti-β1-integrin (MAB 1997; Sigma-Aldrich); mouse anti-thrombospondin (Ab1823; Abcam); guinea pig anti-nephrin (GP-N2; Progen); mouse anti-desmin (sc-23879; Santa Cruz); mouse anti-CD144 (11D4.1; BD Biosciences); mouse anti-WT1 (6F-H2; Sigma-Aldrich); donkey-anti guinea pig IgG antibody horseradish peroxidase (HRP) conjugate (AP193P; Sigma-Aldrich); goat anti-rabbit IgG antibody, (H+L) HRP conjugate (AP307P); rabbit anti-mouse IgG antibody, HRP conjugate (AP160P) (Sigma-Aldrich); goat anti-rat IgG (H+L), Alexa Fluor 488 (A11006; Invitrogen); donkey anti-rabbit IgG (H+L), Alexa Fluor 594 (A21207; Invitrogen); and goat anti-mouse IgG (H+L), Alexa Fluor 488 (A11029; Invitrogen).

Mice

Enriched primary podocytes were isolated using the *Terminator* mouse model as previously published by Guo *et al.* (10). In short, the diphtheria toxin (DT) receptor (DTR) is flanked by loxP sites and introduced into the murine Rosa26 locus. Crossing these *Rosa-DTR^{flox}* mice with *Podocin-Cre*-expressing mice results in expression of the DTR in all murine cells other than podocytes. Addition of DT to the primary kidney cell cultures results in all nonpodocytes being killed, leading to >99% pure podocyte population as per Guo *et al.*, and is in agreement with the immunofluorescence staining for podocyte marker WT1 with DAPI (data not shown). The Yale University Institutional Animal Care & Use Committee approved all animal experiments. All work was carried out in accordance with the principles and procedures outlined in the National Institutes of Health (NIH) guidelines for the care and use of experimental animals.

Quantitative PCR Analysis

Total RNA was extracted from the primary podocytes by using Trizol (Thermo Fisher Scientific). The RNA concentration was measured by spectrophotometry (Nanodrop Technologies). One microgram of total RNA was used for reverse transcription using a high-capacity cDNA Synthesis Kit according to the manufacturer's instructions (Applied Biosystems, Foster City, CA). The quantitative PCR amplifications were performed using Power SYBR green PCR Master Mix (Applied Biosystems) with a 7300 AB real-time PCR machine (Applied Biosystems).

Podocyte Culture

Ten pups of *Podocin-Cre Rosa-DTR^{flox}* mice were sacrificed at 3 days of age. Kidneys were isolated, minced, and digested with 90 μl collagenase A (5 mg/ml) and 10 μl DNase I recombinant for 30 minutes at 37°C. Kidney tissue from each mouse was separately filtered through a 70-μm sieve onto a collagen-coated 10-cm cell culture plate. Cells were incubated overnight and medium was changed the next day. After 48 hours, a confluency of 80% was reached and cells were treated with DT (2 μg/ml stock; Sigma), followed by DT treatment every 48 hours for a total of three times. The resulting pure cultures of primary DTR podocytes were used for experiments 7 days after kidney isolation. Characterization of DTR podocytes was performed by immunoblotting for podocyte markers and markers of other glomerular cells, as previously published by Guo *et al.* (10).

Isolation of CCVs

For proteomic analysis, CCVs from *Podocin-Cre Rosa-DTR^{flox}* mouse podocytes were isolated according to a modified version of "Alternate Protocol 2" in "Isolation of Clathrin-Coated Vesicles by Differential and Density Gradient Centrifugation" by Girard *et al.* (11). Bottles and glass vials were sealed air-tight, and autoclaved before use. All solutions (Supplemental Table 1) were prepared under a cell culture hood. PBS, and buffer A 10× and 1× were filtered twice through a Browning 0.22-μm bottle-top vacuum filter system (Sigma-Aldrich) into new bottles before use. All steps were performed on ice.

Ten collagen-coated 10-cm dishes of DTR podocytes were grown to confluency and used 7 days after kidney isolation. Cells were washed twice with 10 ml room temperature PBS. Next, 550 μl of buffer A 1×, 22 μl of complete protease inhibitor cocktail (Roche), and 2.75 μl of PMSF (1 mg/ml) were added to each dish. The podocytes were scraped off thoroughly with a rubber policeman and combined into 1.5-ml Eppendorf tubes. Homogenization was performed by ten aspirations through a 26 G needle, followed by ten aspirations through a 30 G needle. A 0.5-ml aliquot of this whole-cell lysate was reserved.

The suspension was transferred to 16-ml polycarbonate centrifuge tubes (Thermo Fisher Scientific) and centrifuged for 20 minutes at 20,000 rpm (17,000× *g*) at 4°C in a Sorvall SA-600 rotor using a Sorvall RC 5C Plus Superspeed Centrifuge (Thermo Fisher Scientific). Thereafter, the supernatant (supernatant 1) was transferred into 26.3-ml polycarbonate centrifuge tubes (Beckman).

Supernatant 1 was centrifuged for 2 hours at 28,000 rpm (56,000× *g*) at 4°C in a 60Ti rotor using an Ultracentrifuge Model L8–55M (Beckman). The pellets (P2) were combined in 4.5 ml buffer A 1×, 180 μl complete protease inhibitor

cocktail, and 22.5 μl PMSF, and homogenized with ten aspirations through a 20-G (gauge) needle.

The homogenate was transferred to a 10-ml syringe equipped with a 26-G needle, and was passed through this needle into another ultracentrifuge tube. Then, a 2-mm diameter glass capillary tube was attached to a 5-ml syringe. The syringe barrel was loaded with 5 ml D_2O-sucrose solution and the end of the capillary rested at the bottom of the centrifuge tube containing P2, followed by slow ejection of 2.5 ml D_2O-sucrose solution.

P2 was centrifuged for 2 hours at 42,000 rpm (116,000× *g*) at 4°C in a Ti60 rotor using an Ultracentrifuge Model L8–55M. The resulting pellet (CCVs) was resuspended in 0.25 ml buffer A 1× and transferred to a 1.5-ml Eppendorf tube. Next, 10 μl complete protease inhibitor cocktail and 1.25 μl PMSF were added, and the sample passed ten times through a 30-G needle. Then, 50-μl aliquots of CCVs were transferred into 1.5-ml low-protein binding microcentrifuge tubes (Thermo Fisher Scientific), snap-frozen in liquid nitrogen, and stored at −80°C. Protein concentration was assessed from all aliquots before freezing.

Immunoblotting

Immunoblotting was performed as previously described in our laboratory (5). Briefly, samples were boiled for 5 minutes at 95°C, followed by separation by SDS-PAGE using 4%–20% precast protein gels (Bio-Rad). After transfer, polyvinylidene difluoride membranes were washed twice in TBST (Tris-buffered saline, 0.1% Tween 20) and blocked with 5% dry milk/TBST solution. Membranes were incubated overnight at 4°C with the appropriate primary antibodies diluted in 5% BSA/TBST, followed by washing with TBST three times and incubation with HRP-conjugated secondary antibodies. After washing three times with TBST, signals were detected using enhanced chemiluminescence reagents, Clarity Western ECL Substrate (Bio-Rad), and imaged in an Odyssey Fc (LI-COR Biosciences) using Image Studio.

EM

EM of CCV samples was performed by the Center for Cellular and Molecular Imaging at Yale School of Medicine using the following protocol from Borner *et al.* (12), with their own equipment and materials:

Pelleted fractions were fixed with 2% paraformaldehyde/2.5% glutaraldehyde in 0.1 M cacodylate buffer, pH 7.2, at room temperature for 30 minutes, washed with 0.1 M cacodylate buffer, and postfixed using 1% osmium tetroxide for 1 hour. Pellets were then washed before being incubated with 1% tannic acid in 0.05 M cacodylate buffer, pH 7.2, for 40 minutes to enhance contrast. Pellets were dehydrated in ethanol before being embedded in araldyte CY212 epoxy resin (Agar Scientific, Stansted, UK). Ultrathin sections (70 nm) were cut using a diamond knife mounted on a Reichert Ultracut S ultramicrotome (Leica Microsystems, Milton Keynes, UK) and picked up onto coated EM grids. The sections were stained with lead citrate and observed in a Tecnai Spirit (FEI, Eindhoven, Netherlands) transmission electron microscope at an operating voltage of 80 kV.

MS Analysis

Tandem MS (MS/MS) was carried out by the W.M. Keck Foundation Biotechnology Resource Laboratory at Yale School of Medicine using the following method.

Sample Preparation. First, 10 μl of water was added to the provided protein solution, then reduction was carried out with 2 μl of 45mM dithiothreitol and incubation at 37°C for 20 minutes. Cysteines were then alkylated by the addition of 2 μl of 100 mM iodoacetamide and incubation in the dark at room temperature for 30 minutes. Samples were acetone precipitated by adding 4× the sample volume (100 μl) with precooled acetone at −20°C and vortexed. Solution was then incubated at −20°C overnight, then centrifuged at 14,600× *g* for 10 minutes at 4°C. Supernatant was decanted using a pipette and the protein pellet was resolubilized with 20 μl of a 0.1% RapiGest containing 25 mM ammonium bicarbonate, pH 8. Then, 2 μl of a 0.1 mg/ml trypsin (1/10 of stock; Promega, sequencing grade) was added and the samples were digested at 37°C overnight, and then acidified with 1 μl of 20% trifluoroacetic acid to quench the digestion. Samples were stored at −20°C until just before liquid chromatography (LC)-MS/MS analysis.

LC-MS/MS on the QE-Plus (Thermo Fisher Scientific). Digested samples were injected onto an Orbitrap Fusion (Thermo Fisher Scientific) LC-MS/MS system equipped with a Waters nanoAcquity UPLC system, and a Waters Symmetry C18 180 μm×20 mm trap column and a 1.7 μm, 75 μm×250 mm nanoAcquity UPLC column (37°C) were used for peptide separation. Trapping was done at 5 μl/min with 99% buffer A (100% water and 0.1% formic acid) for 3 minutes. Peptide separation was performed with a linear gradient over 140 minutes at a flow rate of 300 nl/min. MS1 (300–1500 m/z, target value 3E6, and maximum ion injection times 45 ms) were acquired and followed by higher energy collisional dissociation-based fragmentation (normalized collision energy 28). A resolution of 70,000 at m/z 200 was used for MS1 scans, and up to 20 dynamically chosen, most abundant precursor ions were fragmented (isolation window 1.7 m/z). The MS2 scans were acquired at a resolution of 17,500 at m/z 200 (target value 1E5 and maximum ion injection times 100 ms).

The data were processed with either Mascot Distiller (Matrix Science) or Proteome Discoverer (Thermo Fisher Scientific), and protein identification was searched for using the Mascot search algorithm (Matrix Science) using the Mascot search algorithm (Matrix Science) for the June sample submission.

Database Searching. The ".mgf" files were searched in-house using the Mascot algorithm (version 2.4.0) (13) for uninterpreted MS/MS spectra. The data were searched against the SWISSPROT Human protein database (2018-March). Search parameters were as follows:

Type of search: MS/MS Ion Search
Enzyme: Trypsin
Variable modifications: Carbamidomethyl (Cys), Oxidation (Met)
Mass values: Monoisotopic
Protein mass: Unrestricted
Peptide mass tolerance: ±10 ppm
Fragment mass tolerance: ±0.02 Da

Charge: +7
Max missed cleavages: 2
Decoy: Yes
Instrument type: ESI-TRAP

Using the Mascot database search algorithm, proteins were considered identified when Mascot listed them as significant and more than two unique peptides matched the same protein. The Mascot search results were filtered using a false discovery rate of 1% or less for the protein ID.

Analysis of LC-MS Results to Identify Novel Cargo Proteins

Proteins in the LC-MS data set with an expectation value of <0.005 were considered significant and included in further analysis. To identify the most significant cargo proteins, LC-MS results were sorted by Exponentially Modified Protein Abundance Index (emPAI), a score for abundance (14). Proteins ranked higher or equal to "Transferrin receptor protein 1" underwent further analysis. To identify impurities, these proteins were compared with the online supplementary iTRAQ data set S1 from Borner *et al.* (15). Impurities were defined by a control/mock ratio of <1.46, which is the control/mock ratio of "transferrin receptor protein 1." Proteins in our LC-MS results not mentioned in the data set by Borner *et al.* were searched on PubMed for known clathrin association (*Protein name* AND clathrin). *Protein name* was defined as the name in our LC-MS data set or all known names of the human protein homolog according to UniProt (https://www.uniprot.org/). All impurities identified in this manner were excluded. CCV-associated proteins identified in this manner were further searched using PubMed (*Protein name* AND clathrin) to identify their role in CCV trafficking, and categorized either as coat, interactor, or cargo proteins. CCV cargo binding motifs in cargo protein amino acid sequences were identified using the Motif Search of the Kyoto University Bioinformatics Center (https://www.genome.jp/tools/motif/MOTIF2.html).

Immunofluorescence Staining

Primary podocytes grown on collagen I-coated coverslips were washed with PBS and fixed with 4% PFA for 20 minutes, followed by permeabilization with 0.1% Triton X in PBS for 5 minutes. Subsequent blocking was performed with 3% BSA in PBS for 1 hour. Afterward, cells were incubated with primary antibodies overnight at 4°C, followed by incubation with Alexa Fluor 488- and/or Alexa Fluor 594-conjugated secondary antibodies for 1 hour, and washing with PBS. Coverslips were mounted with Slowfade (Invitrogen) and immunofluorescence imaging was performed using an Andor CSU-WDi spinning disc confocal microscope equipped with a Nikon Ti-E Cfi Plan Apo Lambda 60× oil immersion objective. Images were processed using NIH Image J software (version 1.52a) or Adobe Photoshop CS6 Extended.

Results

Enrichment of CCVs from Podocytes

In order to isolate CCVs from cultured DTR podocytes, multiple centrifugation steps were performed culminating in pelleting through a D_2O-sucrose cushion. To first validate the isolated CCVs, we performed ultrastructural examination of the CCV fraction by EM, which revealed an abundance of vesicles among dissociated proteins (Figure 1, A and B). The majority of these vesicles were approximately 100 nm in size and coated by an electron-dense lattice cage, consistent with the morphology of CCVs (16). Next, to determine the enrichment of CCVs, western blotting comparing whole-cell podocyte lysates and the CCV fractions was performed after isolation (Figure 1C). Robust enrichment of the CCV-coat proteins CHC, CLC, and α-adaptin was observed in the CCV fraction when compared with whole-cell lysate. In contrast, the GTPase dynamin was equally expressed in both samples, in line with its temporary association for the fission reaction during clathrin-coated pit internalization from the plasma membrane. As expected, glyceraldehyde 3-phosphate dehydrogenase, used as a negative control, was markedly reduced in the CCV fraction. Together, these observations indicate a strong enrichment of CCVs from podocytes by our isolation protocol.

Identification of Proteins Associated with CCVs by MS

Next, LC-MS was performed to identify proteins in our CCV preparation. A total of 1744 proteins were identified (Supplemental Table 2), of which 1227 were considered

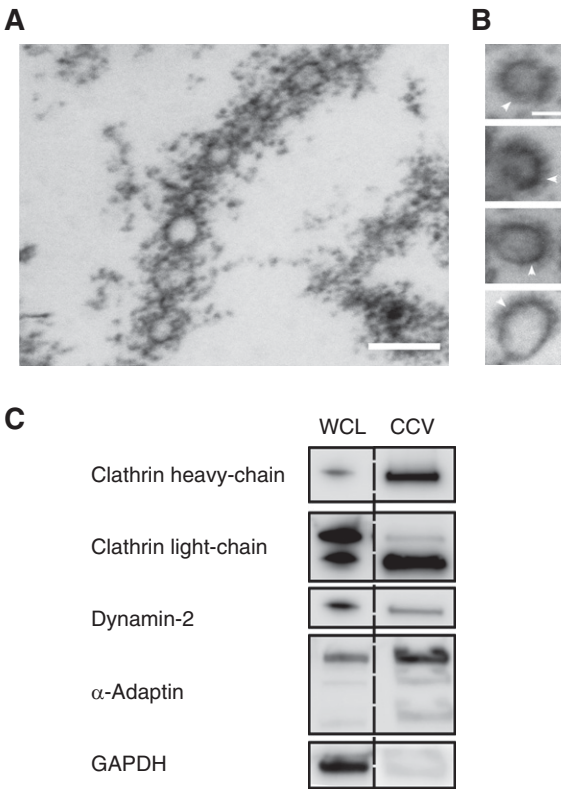

Figure 1. | Enrichment of Clathrin-coated vesicles from podocytes. (A) Electron microscopy image of the CCV fraction from isolated podocytes. Scale bar: 200 nm. (B) Higher-magnification image of single CCVs. Arrowheads indicate the clathrin coat. Scale bar: 50 nm. (C) Immunoblots of podocyte WCL and CCV fractions for clathrin heavy chain, CLC, dynamin-2, α-adaptin, and GAPDH. CCV, clathrin-coated vesicle; CLC, clathrin light chain; GAPDH, glyceraldehyde 3-phosphate dehydrogenase; WCL, whole-cell lysate.

significant with an expectation value of <0.005. CHC was ranked fourth when sorted by Mascot score.

To identify the most abundant cargo proteins in podocytes, we ranked them by abundance according to their emPAI (14). To exclude potential contaminants, because it is difficult to obtain pure isolation of CCVs from cell culture models (2), a multiple-step data analysis approach was implemented (Figure 2A). First, we used a cutoff where proteins more abundant than transferrin receptor protein 1, a classic cargo of CCVs, were examined, totaling 520 proteins (Figure 2B). Then, we compared our candidate proteins with MS results by Borner *et al.* (15) (see their online Supplemental Table 1 at http://jcb.rupress.org/content/175/4/571.long). This group developed a CCV enrichment protocol

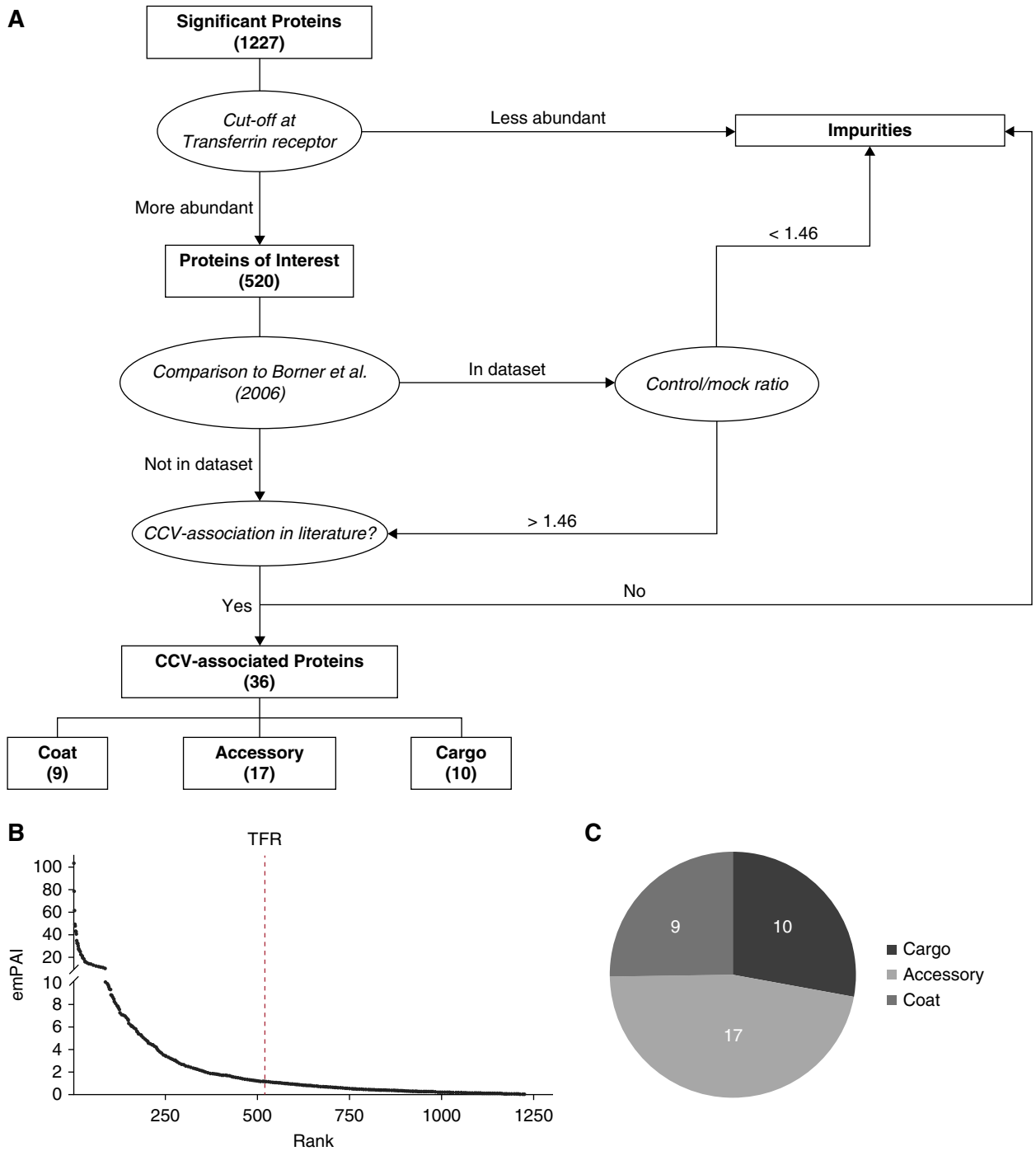

Figure 2. | Identification of cargo proteins by data analysis of LC-MS results. (A) Schematic flowchart demonstrating the protocol used to identify CCV cargo proteins from the vesicle fraction by LC-MS. (B) Proteins by rank and emPAI score with indication of the transferrin receptor as cutoff. (C) Proportion of each category in (A). emPAI, Exponentially Modified Protein Abundance Index; LC-MS, liquid chromatography-mass spectrometry; TFR, transferrin receptor protein.

using both HeLa wild-type cells and HeLa CHC small interfering RNA (siRNA) knockdown cells, resulting in preparation of two fractions: CCVs with contaminants and "mock CCVs," which are solely contaminants because CCVs are not formed in the knockdown model. Next, they performed MS with both preparations and calculated a control/mock ratio for each protein. Thereby, they were able to identify proteins that are genuinely associated with CCVs. We included every protein in our CCV preparation with a control/mock ratio >1.46 for further analysis; the same ratio of transferrin receptor protein 1. A total of 189 proteins from the podocyte CCV data set were identified in the HeLa data set. Of these, 156 had a control/mock ratio of <1.46 and were considered contaminants, while 33 had a ratio of >1.46 (Supplemental Table 2). All proteins identified in this manner and the entire 331 proteins not found in the data set of Borner *et al.* (15) were investigated in the literature for clathrin association. Finally, we were able to identify 36 CCV-associated proteins in our sample (Figure 2C). Of these, 9 are part of the clathrin coat, 17 interact with CCVs, and 10 are cargo proteins.

CCV Coat and Accessory Proteins in Podocytes

Clathrin coat proteins are shown in Table 1. CHCs and CLCs were identified in our sample, with CHCs being the most abundant. In addition, we identified numerous adaptor protein complex proteins that select cargo for CME. AP-2 recognizes cargo at the cell membrane leading to CME and transport from the membrane to the early endosome. AP-1 binds cargo in CCVs that originate from the early endosome and are transported to the trans-Golgi network and late endosome, respectively (17).

Another category of proteins in our sample facilitate the formation and transport of CCVs (Table 2). These accessory proteins include the actin-related protein 2/3 complex (Arp2/3), which propels CCVs from the cell membrane into the cytoplasm by actin polymerization (18,19). Dynactin moves them along microtubules (20). Arf5 and Rab14 mediate CME of specific cargo (21,22), whereas clathrin interactor 1, also known as epsinR, has cargo recognition and additional unknown functions (16). Brain acid soluble protein 1 localizes to CCVs and regulates membrane dynamics (23). Casein kinase 2 phosphorylates CLC and AP-2, mediating initiation of CME (24). Syntaxin 7, as well as vesicle-associated membrane protein (VAMP) 2 and 3, are SNARE proteins that are involved in vesicle fusion and trafficking (25,26).

Cargo Proteins of CCVs in Podocytes

To verify the identified cargo proteins, additional amino acid sequence analysis of murine and human homologs of each cargo protein was performed. Each sequence was examined for the three most common cargo recognition motifs in cell membrane-derived CCVs: YXXø and (DE)XXXL(LI), which are recognized by AP-2, and NPXY, which is recognized by the alternate cargo adaptors Numb, ARH, and Dab2 (17) (Table 3). At least one motif was found in each cargo protein, except for galectin-1. This protein undergoes CME by an unconventional sorting mechanism, involving CD7 and ganglioside GM-1 (27).

Annexin A2 interacts with the μ2-subunit of AP-2 and may function as a transmembrane receptor (28,29). While annexin A2 serves as a cargo of CCVs, its emPAI score in our sample was higher than the emPAI score of CHC (9.67 versus 9.39), indicating that not all annexin A2 in our CCV fraction was bound to CCVs. Nucleolin is primarily found in the nucleus; however, it can translocate to the cell membrane where it functions as an endocytic receptor, where it binds endostatin and lactoferrin, followed by internalization of these proteins through CME (30). Thrombospondin-1 and connective tissue growth factor (CTGF) are internalized through CME after binding to a member of the LDL receptor family (31,32). β1-Integrin is a subunit of a focal adhesion transmembrane receptor that undergoes recycling through CME (33,34). Growth factor receptor-bound protein 10 is an adaptor protein that binds to the IGF-1 and insulin receptor. It forms a complex with NEDD4 that binds to the IGF-1 receptor, followed by CME of this complex-receptor formation (35). Fibronectin-1 undergoes CME after binding to certain receptors, primarily integrins (36,37). Galectin-1 is a soluble β-galactoside-binding protein that undergoes endocytosis through raft- and clathrin-mediated mechanisms (27). The cation-dependent mannose-6-phosphate receptor is a multifunctional transmembrane glycoprotein that undergoes constant recycling through CME (38). Transferrin receptor protein 1 has long been established as a cargo of CCVs (39).

Immunocytochemistry Demonstrates Colocalization of Cargo Proteins and CCVs in Podocytes

To further validate whether the proteins identified in our MS analysis visit clathrin-coated pits, immunofluorescence for CLC and selected cargo proteins was performed in podocytes (Figure 3). Colocalization was observed with

Table 1. CCV coat proteins observed in podocytes

Protein Identifier	Protein Name	Exponentially Modified Protein Abundance Index	Mascot Score	Literature
CLH1	Clathrin heavy chain 1	9.39	7945	(15)
AP-2B1	AP-2 complex subunit β	4.58	2007	(15)
AP-2M1	AP-2 complex subunit μ	3.17	643	(15)
AP-1B1	AP-1 complex subunit β-1	2.93	1673	(17)
AP-2A1	AP-2 complex subunit α-1	2.61	1357	(15)
AP-2A2	AP-2 complex subunit α-2	2.35	1595	(15)
CLCA	Clathrin light chain A	2.09	220	(15)
AP-1G1	AP-1 complex subunit γ-1	1.87	857	(17)
CLCB	Clathrin light chain B	1.68	162	(15)

Table of identified clathrin-coated vesicle coat proteins in podocytes ranked by abundance.

Table 2. Accessory CCV proteins observed in podocytes

Protein Identifier	Protein Name	Exponentially Modified Protein Abundance Index	Mascot Score	Literature
RAB14	Ras-related protein Rab-14	8.49	542	(21)
ARPC3	Actin-related protein 2/3 complex subunit 3	8.09	482	(18,19)
ARPC2	Actin-related protein 2/3 complex subunit 2	6.83	719	(18,19)
ARP3	Actin-related protein 3	5.36	779	(18,19)
ARP2	Actin-related protein 2	3.86	736	(18,19)
ARPC5	Actin-related protein 2/3 complex subunit 5	3.52	270	(18,19)
ARPC4	Actin-related protein 2/3 complex subunit 4	3.34	253	(18,19)
DCTN1	Dynactin subunit 1	2.67	1782	(20)
ARC1B	Actin-related protein 2/3 complex subunit 1B	2.37	506	(18,19)
BASP1	Brain acid soluble protein 1	2.07	587	(23)
STX7	Syntaxin-7	2.05	346	(25,26)
VAMP3	Vesicle-associated membrane protein 3	1.9	385	(25)
VAMP2	Vesicle-associated membrane protein 2	1.63	230	(25)
EPN4	Clathrin interactor 1	1.49	858	(16)
CSK21	Casein kinase II subunit α	1.3	185	(24)
ARF5	ADP-ribosylation factor 5	1.23	116	(22)
DCTN3	Dynactin subunit 3	1.19	205	(20)

Table of identified accessory clathrin-coated vesicle proteins in podocytes ranked by abundance.

proteins such as transferrin receptor protein 1, β1-integrin, and thrombospondin-1, each representing one of the main groups of identified cargo proteins, namely receptors, transmembrane proteins, and extracellular matrix (ECM) proteins.

Discussion

This study marks the first time CCVs from podocytes were isolated and analyzed. We identified 36 CCV-associated proteins in podocytes that were categorized into coat, accessory, and cargo proteins. It has to be noted that syntaxin 7, VAMP2, and VAMP3 were previously considered to be cargo proteins as they are transported inside CCVs to fuse them with target membranes, for example at endosomes (16,40). However, as their main function lies in manipulating the CCV itself, we have decided to categorize them as accessory proteins. Finally, we identified ten novel, highly abundant cargo proteins of CCVs in podocytes.

Table 3. CCV cargo proteins observed in podocytes

Protein Identifier	Protein Name	Exponentially Modified Protein Abundance Index	Mascot Score	NPXY	YXXø	[DE] XXXL[LI]	Literature
ANXA2	Annexin A2	9.67	1277	—	++	++	(28,29)
NUCL	Nucleolin	6.92	3069	—	++	Hsa	(30)
TSP1	Thrombospondin-1	3.01	2243	—	++	++	(31)
CTGF	Connective tissue growth factor	2.73	443	—	++	—	(32)
ITB1	Integrin β-1	1.84	858	++	++	++	(33,34)
GRB10	Growth factor receptor-bound protein 10	1.43	391	—	++	++	(35)
FINC	Fibronectin	1.4	2758	Mmu	++	++	(36,37)
LEG1	Galectin-1	1.28	101	—	—	—	(27)
MPRD	Cation-dependent mannose-6-phosphate receptor	1.22	485	—	++	Mmu	(38)
TFR1	Transferrin receptor protein 1	1.18	640	—	++	Mmu	(39)

Table of identified clathrin-coated vesicle cargo proteins ranked by abundance. Columns "NPXY," "YXXø," and "[DE]XXXL [LI]" show the presence of these cargo recognition motifs in respective protein sequences. "++" indicates presence in human and murine homologs; "Mmu" and "Hsa" indicate presence in a mouse or human homolog, respectively; and "—" indicates the absence of a cargo recognition motif.

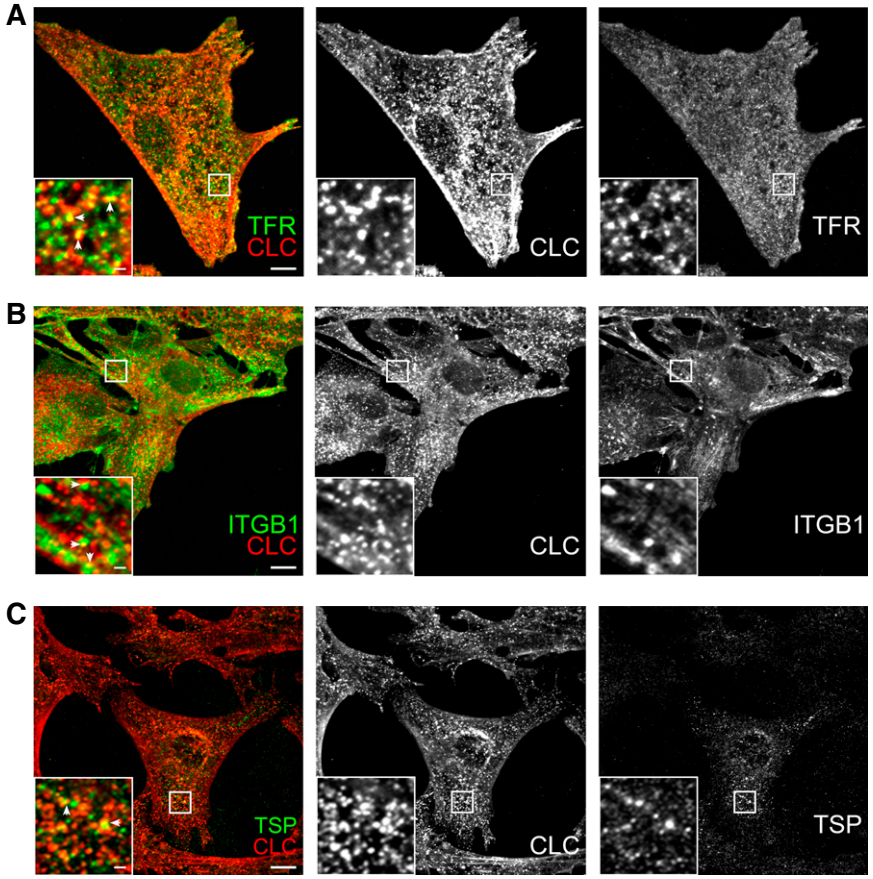

Figure 3. | **Identified CCV cargo proteins colocalize with CCVs in podocytes.** Immunofluorescence of (A) transferrin receptor protein 1 (TFR), (B) β1-integrin (ITGB1), and (C) thrombospondin-1 (TSP) (all green) and CLC (red) in podocytes, at low and high magnification. Arrows indicate colocalization. Scale bar at low magnification: 10 μm; high magnification: 1 μm.

Interestingly, the majority of these proteins have also been implicated in glomerular diseases. The annexin A2–S100A10 complex binds the phospholipase A_2 receptor in podocytes (41). Autoantibodies have been identified against this receptor in most cases of primary membranous nephropathy. Nucleolin binds circulating endostatin, followed by the formation of a complex with α5β1-integrin and the urokinase-type plasminogen activator receptor, ultimately leading to the internalization of endostatin through CME (30). While the function of nucleolin in podocytes requires further investigation, there is evidence for detrimental effects of urokinase-type plasminogen activator receptor-mediated signaling on podocyte health (42). Thrombospondin-1 has been shown to activate TGF-β in diabetic nephropathy, leading to glomerulosclerosis (43), while CTGF is strongly associated with renal fibrosis (44). Furthermore, β1-integrin was identified in CCVs, which, together with different α-subunits, links the podocyte cytoskeleton to the glomerular basement membrane. Knockouts of either subunit α3 or β1-integrin result in profound proteinuria and renal failure in mice (45,46), and human mutations in α3-integrin have been associated with early onset nephrotic syndrome (47). In addition, the importance of β1-integrin has been validated by interacting proteins such as talin-1, because loss of this gene phenocopies loss of β1-integrin (48). Fibronectin-1 accumulation leads to glomerulosclerosis (49), and galectin-1 upregulation in podocytes is associated with diabetic nephropathy because it binds the ectodomain of nephrin and might function as a slit diaphragm component (50). Lastly, there is evidence that glycated transferrin accumulates in podocytes in diabetic nephropathy, leading to podocyte damage and progression of proteinuric kidney disease (51). After podocyte CCV isolation, the only identified cargo protein without known function or interaction with implications for podocyte health is the cation-dependent mannose-6-phosphate receptor.

Thus far, CCV proteomes have been created from rat liver and brain tissue, as well as HeLa cells (12). Our analysis of CCVs from podocytes represents, to our knowledge, the first time that this has been performed in specific cells. Because the approaches to protein identification differ in all published CCV proteomes, it is difficult to compare our findings directly with previous results such as the brain (52) and liver (53) CCV proteomes, which were published in 2004 and 2005, respectively. In these early papers, the authors did not use an unbiased approach like Borner *et al.* (15), resulting in numerous likely "false-positive" CCV-associated proteins (15). Examples are proteins involved in glycolysis, which were deemed contaminants in later publications. There are some similarities between CCVs from podocytes and other cells. In particular, coat proteins, such as AP-1, AP-2, and clathrin, as well as

accessory proteins like syntaxins, VAMPs, and other proteins associated with CCV assembly and transport are common among all (40,52,53); however, they differ to some degree in their cargo proteins. Brain CCVs are strongly associated with synaptic vesicle proteins (52). While the transferrin receptor was not identified in brain CCVs, it has been observed in liver, HeLa, and podocyte CCVs. Interestingly, liver CCVs contain asialoglycoprotein receptors, ferritin, and the hepatic glucose transport receptor, which play important roles in liver metabolism (53). The cargo of HeLa cell CCVs is comprised largely of lysosomal proteins like DNase 2, different hydrolases, and cathepsins (40). Interestingly, these were either absent or ranked very low in podocyte and tissue CCVs. In fact, only cathepsin D was identified in podocyte CCVs with an emPAI score of 0.32, while the transferrin receptor had an emPAI score of 1.18.

The transferrin receptor and cation-dependent mannose-6-phosphate receptor were found in CCVs from podocytes and other cells. However, other classic CCV cargo proteins seem to play a minor role in podocytes. For example, the epidermal growth factor receptor is entirely missing, while the LDL-receptor and cation-independent mannose-6-phosphate receptor are of extremely low abundance in podocyte CCVs, with emPAI scores of 0.14 and 0.06, respectively. Our identified podocyte CCV cargo is somewhat unique in that it is mainly made up of receptors, transmembrane proteins, and ECM proteins. In particular, the abundance of ECM proteins like thrombospondin-1 and fibronectin is interesting, and implicates matrix regulation by podocytes. There are some limitations as we are using a model of podocytes in culture, so some cargo proteins that have detrimental effects on podocytes, like CTGF, thrombospondin-1, and fibronectin, may not be highly expressed in healthy glomeruli *in vivo*. However, the ability of podocytes to endocytose these proteins might play a role in the initial steps of glomerular disease or function as an adaptive protective response. As demonstrated by the above-mentioned manuscripts, the current knowledge of CCV-associated proteins is constantly evolving. For this reason, we searched the literature for CCV-association for each candidate protein as part of our data analysis to additionally identify proteins that have not been recognized as CCV-associated by Borner *et al.* (15).

The degree of sample purity is crucial for the interpretation of MS results. In this study, precautions were taken to avoid contamination of samples with human material. Indeed, not a single human peptide was found on MS, supporting the importance of sterile working conditions. The biggest challenge in analyzing proteomic analysis of CCVs is to distinguish genuine CCV-associated proteins from contaminants. For this reason, it was important to assess the amounts of CCV-associated proteins among all proteins in our preparation. We identified 36 CCV-associated proteins from 520 candidates, representing a fraction of about 6.9%, which is similar to the results of Borner *et al.* (15) that reported a yield of 10.1% CCV-associated proteins in their sample. A highly abundant group of contaminants in our sample were proteins of ribosomal or RNA-binding origin, which were again similarly abundant in the results of Borner *et al.* (15). RNA granules cofractionate with CCVs during sample preparation owing to similar density and size, resulting in these findings (52). Distinguishing between contaminants and genuine CCV proteins can be achieved by either obtaining a large yield of CCVs by enrichment from whole tissue, or by comparing an siRNA clathrin knockdown to wild-type culture cells. Yet, when creating a CCV proteome from enriched primary podocytes, these approaches are less applicable. Podocytes only represent a small number of all kidney cells, so CCV isolation from whole kidney tissue is not specific. Moreover, transfection, viral infection, or nucleofection efficiency in podocytes is low in comparison to HeLa cells (54), so a clathrin siRNA knockdown may not be sufficient to provide a significant difference in CCV assembly. Therefore, we created a partial CCV proteome from podocytes by using an approach with high specificity to decrease the amount of false-positives. The transferrin receptor is a well documented, highly conserved CCV cargo protein and was chosen as a useful, albeit arbitrary, cutoff to focus on the most abundant and thus mostly enriched proteins. While this excluded around 700 lower-ranked peptides, their individual abundance was minimal in comparison to the first 520, indicating lack of enrichment with CCVs (Figure 2B). To further increase specificity, our approach included eliminating previously identified impurities, peptide sequence analysis, and conducting a literature review. Yet, a caveat of our approach is a reduced sensitivity. Certain CCV-associated proteins in Borner *et al.* (15), for example dynamin-2, were not adequately enriched to meet our threshold. However, these proteins are only briefly associated with CCVs, so they may not affect our primary goal of identifying cargo proteins. Of course, there is the possibility that previously unknown CCV cargo proteins whose CCV association has not yet been described in the literature are observed in our data set. Collectively, our experimental design allowed us to exclude all contaminants from our readout and identify genuine CCV cargo proteins with high confidence.

It is worth noting that podocyte cell culture has some limitations. For example, the slit diaphragm protein nephrin, a prominent and established cargo protein of CCVs in podocytes (4), was absent from our LC-MS results. Only CD2AP and podocalyxin were identified by LC-MS, although with nonsignificant expectation values. This is a well known limitation of the podocyte *in vitro* model, because well established podocyte markers are not always expressed or lose expression over time when compared with whole kidneys (55). Further corroborating this finding, nephrin expression was lost in DT-treated podocytes in comparison to whole kidney lysates from *Podocin-Cre Rosa-DTR^{flox}* mice. Yet, we were able to characterize our cultured podocytes through positivity for the nuclear podocyte marker WT1 which was enriched by quantitative PCR and immunoblotting (Supplemental Figure 1, A and B), and the absence of endothelial and mesangial cell markers on immunoblot (Supplemental Figure 1B).

Despite the lack of classic slit diaphragm proteins, our results greatly augment the corpus of known internalized proteins in podocytes. These terminally differentiated cells rely heavily on homeostasis of their environment, while disruption leads to cellular damage. We postulate that the endocytosis of the identified cargo proteins provides a method to regulate and maintain a properly functioning glomerular environment. Taken together, we identified, for the first time, highly abundant novel cargo proteins in podocytes

that lay the groundwork for motivating further research on the effect of these proteins on glomerular health.

Acknowledgments

We thank W. W. Wang and J. Kanyo from the Keck MS and Proteomics Resource at Yale for the MS sample preparation, and data collection and analysis, respectively.

This work was performed in fulfillment of the requirements for obtaining the degree Doctor of Medicine (Dr. med.) by M. Groener.

Author Contributions

M. Groener and S. Ishibe conceptualized the study; M. Groener was responsible for data curation, validation , and visualization; M. Groener, K. Inoue, S. Ishibe, C. Pedigo, M. Schiffer, and X. Tian were responsible for formal analysis; E. Baik, E. Cross, K. Ebenezer, M. Groener, and Y. Wang were responsible for investigation; E. Cross, M. Groener, K. Inoue, C. Pedigo, X. Tian, and Y. Wang were responsible for methodology; S. Ishibe was responsible for funding acquisition, project administration, and resources; K. Inoue, S. Ishibe, and M. Schiffer were responsible for supervision; M. Groener and S. Ishibe were responsible for writing the original draft; E. Cross, M. Groener, K. Inoue, S. Ishibe, C. Pedigo, M. Schiffer, X. Tian, and Y. Wang were responsible for reviewing and editing the manuscript. All authors approved the final version of the manuscript.

Disclosures

All authors have nothing to disclose.

Funding

This work was supported in part by the George O'Brien Kidney Center at Yale *via* grant P30 DK-078310, National Institutes of Health (NIH) grants DK-083294 and DK-093629 (to S. Ishibe), and Department of Defense grant W81XWH-17-1-0662. M. Groener was supported by TRENAL, a Deutscher Akademischer Austauschdienst thematic network grant. The Orbitrap Fusion LC MS/MS mass spectrometer system was funded by NIH Shared Instrumentation grant 1S10ODOD018034 and Yale School of Medicine.

Supplemental Material

This article contains supplemental material online at http://kidney360.asnjournals.org/lookup/suppl/doi:10.34067/KID.K3602020000021/-/DCSupplemental.

Supplemental Table 1. Buffer composition for CCV isolation protocol.

Supplemental Table 2. Podocyte CCV LC-MS results and comparison to the published HeLa cell CCV proteome.

Supplemental Figure 1. Validation of enriched DTR-podocytes.

References

1. McMahon HT, Boucrot E: Molecular mechanism and physiological functions of clathrin-mediated endocytosis. *Nat Rev Mol Cell Biol* 12: 517–533, 2011
2. McPherson PS: Proteomic analysis of clathrin-coated vesicles. *Proteomics* 10: 4025–4039, 2010
3. Farquhar MG, Vernier RL, Good RA: An electron microscope study of the glomerulus in nephrosis, glomerulonephritis, and lupus erythematosus. *J Exp Med* 106: 649–660, 1957
4. Soda K, Ishibe S: The function of endocytosis in podocytes. *Curr Opin Nephrol Hypertens* 22: 432–438, 2013
5. Soda K, Balkin DM, Ferguson SM, Paradise S, Milosevic I, Giovedi S, Volpicelli-Daley L, Tian X, Wu Y, Ma H, Son SH, Zheng R, Moeckel G, Cremona O, Holzman LB, De Camilli P, Ishibe S: Role of dynamin, synaptojanin, and endophilin in podocyte foot processes. *J Clin Invest* 122: 4401–4411, 2012
6. Hermle T, Schneider R, Schapiro D, Braun DA, van der Ven AT, Warejko JK, Daga A, Widmeier E, Nakayama M, Jobst-Schwan T, Majmundar AJ, Ashraf S, Rao J, Finn LS, Tasic V, Hernandez JD, Bagga A, Jalalah SM, El Desoky S, Kari JA, Laricchia KM, Lek M, Rehm HL, MacArthur DG, Mane S, Lifton RP, Shril S, Hildebrandt F: *GAPVD1* and *ANKFY1* mutations implicate RAB5 regulation in nephrotic syndrome. *J Am Soc Nephrol* 29: 2123–2138, 2018
7. Dorval G, Kuzmuk V, Gribouval O, Welsh GI, Bierzynska A, Schmitt A, Miserey-Lenkei S, Koziell A, Haq S, Benmerah A, Mollet G, Boyer O, Saleem MA, Antignac C: TBC1D8B loss-of-function mutations lead to X-linked nephrotic syndrome via defective trafficking pathways. *Am J Hum Genet* 104: 348–355, 2019
8. Quack I, Woznowski M, Potthoff SA, Palmer R, Königshausen E, Sivritas S, Schiffer M, Stegbauer J, Vonend O, Rump LC, Sellin L: PKC alpha mediates beta-arrestin2-dependent nephrin endocytosis in hyperglycemia. *J Biol Chem* 286: 12959–12970, 2011
9. Inoue K, Tian X, Velazquez H, Soda K, Wang Z, Pedigo CE, Wang Y, Cross E, Groener M, Shin JW, Li W, Hassan H, Yamamoto K, Mundel P, Ishibe S: Inhibition of endocytosis of clathrin-mediated angiotensin II receptor type 1 in podocytes augments glomerular injury. *J Am Soc Nephrol* 30: 2307–2320, 2019
10. GuoJ-K, Shi H, Koraishy F, Marlier A, Ding Z, Shan A, Cantley LG: The Terminator mouse is a diphtheria toxin-receptor knock-in mouse strain for rapid and efficient enrichment of desired cell lineages. *Kidney Int* 84: 1041–1046, 2013
11. Girard M, Allaire PD, Blondeau F, McPherson PS: Isolation of clathrin-coated vesicles by differential and density gradient centrifugation. *Curr Protoc Cell Biol* 26: 3.13.1–3.13.31, 2001
12. Borner GH, Hein MY, Hirst J, Edgar JR, Mann M, Robinson MS: Fractionation profiling: A fast and versatile approach for mapping vesicle proteomes and protein-protein interactions. *Mol Biol Cell* 25: 3178–3194, 2014
13. Hirosawa M, Hoshida M, Ishikawa M, Toya T: MASCOT: Multiple alignment system for protein sequences based on three-way dynamic programming. *Comput Appl Biosci* 9: 161–167, 1993
14. Ishihama Y, Oda Y, Tabata T, Sato T, Nagasu T, Rappsilber J, Mann M: Exponentially modified protein abundance index (emPAI) for estimation of absolute protein amount in proteomics by the number of sequenced peptides per protein. *Mol Cell Proteomics* 4: 1265–1272, 2005
15. Borner GH, Harbour M, Hester S, Lilley KS, Robinson MS: Comparative proteomics of clathrin-coated vesicles. *J Cell Biol* 175: 571–578, 2006
16. Hirst J, Edgar JR, Borner GHH, Li S, Sahlender DA, Antrobus R, Robinson MS: Contributions of epsinR and gadkin to clathrin-mediated intracellular trafficking. *Mol Biol Cell* 26: 3085–3103, 2015
17. Sanger A, Hirst J, Davies AK, Robinson MS: Adaptor protein complexes and disease at a glance. *J Cell Sci* 132: jcs222992, 2019
18. Kaksonen M, Toret CP, Drubin DG: Harnessing actin dynamics for clathrin-mediated endocytosis. *Nat Rev Mol Cell Biol* 7: 404–414, 2006
19. Merrifield CJ, Qualmann B, Kessels MM, Almers W: Neural Wiskott Aldrich Syndrome Protein (N-WASP) and the Arp2/3 complex are recruited to sites of clathrin-mediated endocytosis in cultured fibroblasts. *Eur J Cell Biol* 83: 13–18, 2004
20. Zhao Y, Gaidarov I, Keen JH: Phosphoinositide 3-kinase C2alpha links clathrin to microtubule-dependent movement. *J Biol Chem* 282: 1249–1256, 2007
21. Su H, Liu B, Fröhlich O, Ma H, Sands JM, Chen G: Small GTPase Rab14 down-regulates UT-A1 urea transport activity through enhanced clathrin-dependent endocytosis. *FASEB J* 27: 4100–4107, 2013
22. Moravec R, Conger KK, D'Souza R, Allison AB, Casanova JE: BRAG2/GEP100/IQSec1 interacts with clathrin and regulates $\alpha 5\beta 1$ integrin endocytosis through activation of ADP ribosylation factor 5 (Arf5). *J Biol Chem* 287: 31138–31147, 2012
23. Ueno S, Miyoshi H, Maruyama Y, Morita M, Maekawa S: Interaction of dynamin I with NAP-22, a neuronal protein enriched in the presynaptic region. *Neurosci Lett* 675: 59–63, 2018

24. Delom F, Fessart D: Role of phosphorylation in the control of clathrin-mediated internalization of GPCR. *Int J Cell Biol* 2011: 246954, 2011
25. Miller SE, Sahlender DA, Graham SC, Höning S, Robinson MS, Peden AA, Owen DJ: The molecular basis for the endocytosis of small R-SNAREs by the clathrin adaptor CALM. *Cell* 147: 1118–1131, 2011
26. Prekeris R, Yang B, Oorschot V, Klumperman J, Scheller RH: Differential roles of syntaxin 7 and syntaxin 8 in endosomal trafficking. *Mol Biol Cell* 10: 3891–3908, 1999
27. Fajka-Boja R, Blaskó A, Kovács-Sólyom F, Szebeni GJ, Tóth GK, Monostori E: Co-localization of galectin-1 with GM1 ganglioside in the course of its clathrin- and raft-dependent endocytosis. *Cell Mol Life Sci* 65: 2586–2593, 2008
28. Creutz CE, Snyder SL: Interactions of annexins with the mu subunits of the clathrin assembly proteins. *Biochemistry* 44: 13795–13806, 2005
29. Bharadwaj A, Bydoun M, Holloway R, Waisman D: Annexin A2 heterotetramer: Structure and function. *Int J Mol Sci* 14: 6259–6305, 2013
30. Song N, Ding Y, Zhuo W, He T, Fu Z, Chen Y, Song X, Fu Y, Luo Y: The nuclear translocation of endostatin is mediated by its receptor nucleolin in endothelial cells. *Angiogenesis* 15: 697–711, 2012
31. Greenaway J, Lawler J, Moorehead R, Bornstein P, Lamarre J, Petrik J: Thrombospondin-1 inhibits VEGF levels in the ovary directly by binding and internalization via the low density lipoprotein receptor-related protein-1 (LRP-1). *J Cell Physiol* 210: 807–818, 2007
32. Kawata K, Kubota S, Eguchi T, Aoyama E, Moritani NH, Kondo S, Nishida T, Takigawa M: Role of LRP1 in transport of CCN2 protein in chondrocytes. *J Cell Sci* 125: 2965–2972, 2012
33. ChaoW-T, Ashcroft F, Daquinag AC, Vadakkan T, Wei Z, Zhang P, Dickinson ME, Kunz J: Type I phosphatidylinositol phosphate kinase beta regulates focal adhesion disassembly by promoting beta1 integrin endocytosis. *Mol Cell Biol* 30: 4463–4479, 2010
34. Bridgewater RE, Norman JC, Caswell PT: Integrin trafficking at a glance. *J Cell Sci* 125: 3695–3701, 2012
35. Monami G, Emiliozzi V, Morrione A: Grb10/Nedd4-mediated multiubiquitination of the insulin-like growth factor receptor regulates receptor internalization. *J Cell Physiol* 216: 426–437, 2008
36. Altankov G, Grinnell F: Fibronectin receptor internalization and AP-2 complex reorganization in potassium-depleted fibroblasts. *Exp Cell Res* 216: 299–309, 1995
37. Klinger MH, Klüter H: Immunocytochemical colocalization of adhesive proteins with clathrin in human blood platelets: Further evidence for coated vesicle-mediated transport of von Willebrand factor, fibrinogen and fibronectin. *Cell Tissue Res* 279: 453–457, 1995
38. Ghosh P, Dahms NM, Kornfeld S: Mannose 6-phosphate receptors: New twists in the tale. *Nat Rev Mol Cell Biol* 4: 202–212, 2003
39. Harding C, Heuser J, Stahl P: Receptor-mediated endocytosis of transferrin and recycling of the transferrin receptor in rat reticulocytes. *J Cell Biol* 97: 329–339, 1983
40. Borner GHH, Antrobus R, Hirst J, Bhumbra GS, Kozik P, Jackson LP, Sahlender DA, Robinson MS: Multivariate proteomic profiling identifies novel accessory proteins of coated vesicles. *J Cell Biol* 197: 141–160, 2012
41. Fresquet M, Jowitt TA, McKenzie EA, Ball MD, Randles MJ, Lennon R, Brenchley PE: PLA_2R binds to the annexin A2-S100A10 complex in human podocytes. *Sci Rep* 7: 6876, 2017
42. Wei C, Möller CC, Altintas MM, Li J, Schwarz K, Zacchigna S, Xie L, Henger A, Schmid H, Rastaldi MP, Cowan P, Kretzler M, Parrilla R, Bendayan M, Gupta V, Nikolic B, Kalluri R, Carmeliet P, Mundel P, Reiser J: Modification of kidney barrier function by the urokinase receptor. *Nat Med* 14: 55–63, 2008
43. Daniel C, Schaub K, Amann K, Lawler J, Hugo C: Thrombospondin-1 is an endogenous activator of TGF-beta in experimental diabetic nephropathy *in vivo*. *Diabetes* 56: 2982–2989, 2007
44. Yokoi H, Mukoyama M: Analysis of pathological activities of CCN proteins in fibrotic diseases: Kidney fibrosis. *Methods Mol Biol* 1489: 431–443, 2017
45. Pozzi A, Jarad G, Moeckel GW, Coffa S, Zhang X, Gewin L, Eremina V, Hudson BG, Borza DB, Harris RC, Holzman LB, Phillips CL, Fassler R, Quaggin SE, Miner JH, Zent R: Beta1 integrin expression by podocytes is required to maintain glomerular structural integrity. *Dev Biol* 316: 288–301, 2008
46. Sachs N, Kreft M, van den Bergh Weerman MA, Beynon AJ, Peters TA, Weening JJ, Sonnenberg A: Kidney failure in mice lacking the tetraspanin CD151. *J Cell Biol* 175: 33–39, 2006
47. Has C, Spartà G, Kiritsi D, Weibel L, Moeller A, Vega-Warner V, Waters A, He Y, Anikster Y, Esser P, Straub BK, Hausser I, Bockenhauer D, Dekel B, Hildebrandt F, Bruckner-Tuderman L, Laube GF: Integrin $\alpha 3$ mutations with kidney, lung, and skin disease. *N Engl J Med* 366: 1508–1514, 2012
48. Tian X, Kim JJ, Monkley SM, Gotoh N, Nandez R, Soda K, Inoue K, Balkin DM, Hassan H, Son SH, Lee Y, Moeckel G, Calderwood DA, Holzman LB, Critchley DR, Zent R, Reiser J, Ishibe S: Podocyte-associated talin1 is critical for glomerular filtration barrier maintenance. *J Clin Invest* 124: 1098–1113, 2014
49. Zhu L, QiX-Y, Aoudjit L, Mouawad F, Baldwin C, Nattel S, Takano T: Nuclear factor of activated T cells mediates RhoA-induced fibronectin upregulation in glomerular podocytes. *Am J Physiol Renal Physiol* 304: F849–F862, 2013
50. Shimizu M, Khoshnoodi J, Akimoto Y, Kawakami H, Hirano H, Higashihara E, Hosoyamada M, Sekine Y, Kurayama R, Kurayama H, Joh K, Hirabayashi J, Kasai K, Tryggvason K, Ito N, Yan K: Expression of galectin-1, a new component of slit diaphragm, is altered in minimal change nephrotic syndrome. *Lab Invest* 89: 178–195, 2009
51. Gonzalez S, Vargas L: Diabetogenic transferrin damages podocytes in early human diabetic nephropathy. *Horm Metab Res* 33: 84–88, 2001
52. Blondeau F, Ritter B, Allaire PD, Wasiak S, Girard M, Hussain NK, Angers A, Legendre-Guillemin V, Roy L, Boismenu D, Kearney RE, Bell AW, Bergeron JJ, McPherson PS: Tandem MS analysis of brain clathrin-coated vesicles reveals their critical involvement in synaptic vesicle recycling. *Proc Natl Acad Sci U S A* 101: 3833–3838, 2004
53. Girard M, Allaire PD, McPherson PS, Blondeau F: Non-stoichiometric relationship between clathrin heavy and light chains revealed by quantitative comparative proteomics of clathrin-coated vesicles from brain and liver. *Mol Cell Proteomics* 4: 1145–1154, 2005
54. Shankland SJ, Pippin JW, Reiser J, Mundel P: Podocytes in culture: Past, present, and future. *Kidney Int* 72: 26–36, 2007
55. Yaoita E, Yoshida Y, Nameta M, Takimoto H, Fujinaka H: Induction of interdigitating cell processes in podocyte culture. *Kidney Int* 93: 519–524, 2018

Received: January 16, 2020 **Accepted:** April 13, 2020